Clim Dyn
DOI 10.1007/s00382-013-1770-4

Observational estimate of climate sensitivity from changes in the rate of ocean heat uptake and comparison to CMIP5 models

Troy Masters

Received: 17 December 2012 / Accepted: 9 April 2013

Abstract Climate sensitivity is estimated based on 0–2,000 m ocean heat content and surface temperature observations from the second half of the 20th century and first decade of the 21st century, using a simple energy balance model and the change in the rate of ocean heat uptake to determine the radiative restoration strength over this time period. The relationship between this 30–50 year radiative restoration strength and longer term effective sensitivity is investigated using an ensemble of 32 model configurations from the Coupled Model Intercomparison Project phase 5 (CMIP5), suggesting a strong correlation between the two. The mean radiative restoration strength over this period for the CMIP5 members examined is 1.16 $Wm^{-2}K^{-1}$, compared to 2.05 $Wm^{-2}K^{-1}$ from the observations. This suggests that temperature in these CMIP5 models may be too sensitive to perturbations in radiative forcing, although this depends on the actual magnitude of the anthropogenic aerosol forcing in the modern period. The potential change in the radiative restoration strength over longer timescales is also considered, resulting in a likely (67 %) range of 1.5–2.9 K for equilibrium climate sensitivity, and a 90 % confidence interval of 1.2–5.1 K.

Keywords Climate sensitivity · Ocean heat uptake · CMIP model sensitivity · Climate feedback

1 Introduction

Equilibrium Climate Sensitivity (ECS) is a metric commonly used to describe the relationship between temperature and an imposed radiative forcing. It refers to the increase in temperature that could be expected from instantaneously doubling the concentration of atmospheric CO_2 and allowing the system to achieve radiative equilibrium at the top of the atmosphere (TOA). Determining this sensitivity for the actual earth system is important, particularly with respect to potential warming in the coming centuries. Many methods have thus been employed to estimate this value (Annan and Hargreaves 2006; Knutti and Hegerl 2008), either from palaeorecords (Edwards et al. 2007), atmosphere–ocean coupled general circulation model (AOGCM) ensembles (Murphy et al. 2004), or the more recent evolution of climate observations (Lin et al. 2010; Schwartz 2012; Aldrin et al. 2012).

A simple linear energy balance model to describe the relationship between temperature and forcing at TOA is:

$$\Delta N = \Delta F - \lambda(\Delta T) \quad (1)$$

where N is the net downward TOA radiative flux, F is the TOA forcing, and $\lambda(\Delta T)$ is the outgoing TOA radiative response resulting from the strength of radiative restoration (λ) and the change in surface temperature (ΔT). Clearly, the climate temperature sensitivity will thus be inversely related to λ. Assuming a constant value for λ across all timescales would make ECS a simple calculation ($\Delta F_{2xCO2}/\lambda$), but there is evidence to suggest that λ varies based on the timescale, at least in several AOGCMs (Winton et al. 2010; Held et al. 2010; Armour et al. 2012).

In particular, it is questionable whether the λ diagnosed from the inter-annual fluctuations caused by internal dynamics such as ENSO provides a good estimate for the value of λ on longer timescales (Lin et al. 2011; Colman and Hanson 2012). Nevertheless, several groups have estimated λ from short periods of satellite-observed changes in TOA flux (Forster and Gregory 2006; Murphy et al.

T. Masters (✉)
Los Angeles, CA, USA
e-mail: tmasters@ucla.edu

Published online: 17 April 2013

2009; Lindzen and Choi 2011), as there does not exist a satellite record extending the length of what would be considered a "climate scale" (e.g., 30+ years) time span.

In place of satellite observations, it is possible to estimate the change in TOA radiative flux (ΔN) based upon the change in the rate of ocean heat uptake between two periods (Gregory et al. 2002), as the ocean absorbs the vast majority of the excess energy over a long-term TOA imbalance (Levitus et al. 2012). This provides the advantage of having a longer record for N than provided by satellites, and is thus the method chosen here.

This paper is organized as follows: Sect. 2 focuses on the strength of radiative restoration ($\lambda_{50\mathrm{yr}}$) for the latter part of the 20th century and early part of the 21st century as diagnosed from observations over that time period. Section 3 focuses on the relationship between $\lambda_{50\mathrm{yr}}$ and λ_{eff} in the Coupled Model Intercomparison Project phase 5 (CMIP5) model runs, where λ_{eff} is the effective radiative restoration strength as calculated from the pre-industrial state through 2,100 in the Representative Concentration Pathways (RCP) 4.5 scenario, and additionally compares the CMIP5 model results to the range of values obtained in Sect. 2. Section 4 focuses on estimating the underlying equilibrium climate sensitivity from these quantities, and Sect. 5 provides discussion of these values within the context of other estimates and the CMIP5 models examined.

2 Historical radiative restoration strength

Although the exact length of time varies depending on which start year is picked, the radiative restoration strength as determined from the historical ocean heat content (OHC), forcing estimate, and surface temperature will be referred to here as $\lambda_{50\mathrm{yr}}$.

2.1 Data and methods

2.1.1 *TOA net radiative flux*

The ocean heat content data used for the main analysis comes from Levitus et al. (2012) for the 0–2,000 m layer. Over each period, the net TOA flux can be determined as follows:

$$N \times \beta = \frac{dH}{dt} \tag{2}$$

where H is the ocean heat content and β is the percent of the TOA imbalance flux during the period taken up by the ocean's 0–2,000 m layer. Annual data is provided for the most recent 8 years of OHC due to the vast increase in float coverage, which allows us to use this latest data as an 8-year average heat flux into the ocean that forms the basis for one "current" TOA imbalance (N_{cur}) data point. Prior to that, only pentadal averages for OHC are available, in which case by differencing we can use three independent pentadal averages to determine a 10-year average flux into the ocean (used for other N_{cur} data points and N_{hist}). As even the pentadal average OHC contains large error bounds, and β itself may vary across periods, the median value and confidence interval for N over different periods are bootstrapped from Monte Carlo simulation (Fig. 1a). The OHC for each period is drawn from a Gaussian distribution using the mean value and standard error provided by Levitus et al. (2012), and β is drawn from a uniform distribution between 85 and 95 % for each period. The resulting best estimates based on this approach for the current TOA imbalance from 2005 to 2012 is 0.49 Wm^{-2}, which coincides well with other estimates for TOA imbalance over the last decade (Loeb et al. 2012).

Additionally, two other datasets for upper ocean heat content (UOHC) are considered, given that the choice of this OHC dataset can strongly influence estimates of sensitivity (Mascioli et al. 2012). One dataset comes from Domingues et al. (2008) and the other from Ishii and Kimoto (2009), with both having been updated to include data for recent years. Similar to Church et al. (2011), the upper ocean heat content (0–700 m) for these is combined with the lower ocean (700–2,000 m) from Levitus et al. (2012), although as this method relies on the change in ocean heat uptake, the actual pentadal average for 700–2,000 m is used for each period rather than simply a linear trend throughout the record. Since all these resulting estimates thus use the same 700–2,000 m ocean heat content data they cannot be considered independent, but as only about one-third of the warming occurs in this deeper layer in the Levitus data, comparing estimates using the UOHC estimated from different groups does provide an additional check. Due to the non-trivial nature of determining uncertainty in the 0–2,000 m layer for these heterogeneous sets, only point estimates are produced for the analysis using the Domingues and Ishii and Kimoto UOHC sets. Using Ishii and Kimoto (2009), the best estimate for recent imbalance is 0.45 Wm^{-2}, similar to the Levitus dataset, whereas using Domingues dataset yields a best estimate over this period of 0.72 Wm^{-2}, which is on the high side relative to other estimates.

2.1.2 *Historical forcing data*

The primary historical radiative forcing data used here comes from the effective forcings as calculated by GISS Model-E (Hansen et al. 2007). While most of these are well-constrained over this period and consistent across modeling efforts, the magnitude of the direct and indirect

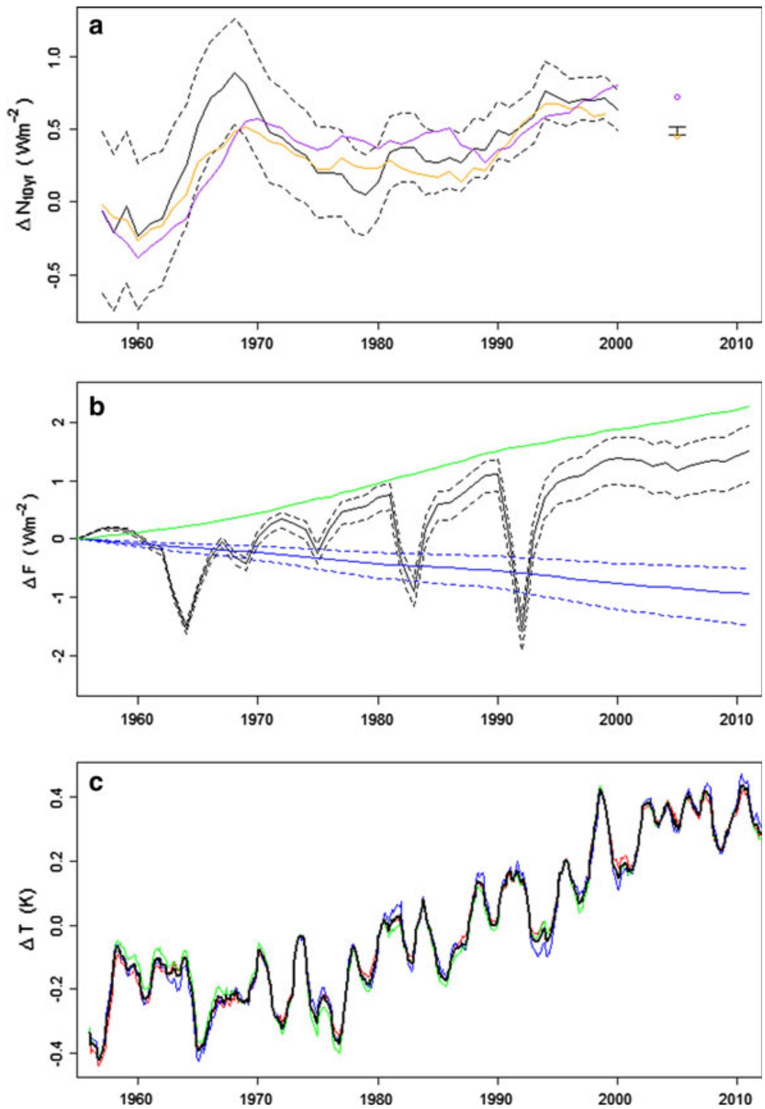

Fig. 1 **a** The median (*solid black*) and 2.5–97.5 % interval (*dashed black*) for decadal average TOA imbalance (N_{hist}) as derived from Levitus et al. (2012) OHC 0–2,000 m pentadal historical data, as well as the confidence interval for the most recent 8-year period from annual data (N_{cur}). Decadal average TOA imbalance also shown for when Domingues et al. (*purple*) and Ishii and Kimoto (*orange*) UOHC data are used. **b** The median (*solid back*) and 2.5–97.5 % interval (*dashed back*) annual total forcing change from 1955, along with median (*solid blue*) and 2.5–97.5 % interval (*dashed blue*) for annual anthropogenic aerosol change and estimated forcing change for long-lived greenhouse gases (*green*) relative to 1955. **c** The 12-month running mean surface temperature anomalies from NCDC (*red*), GISS (*blue*), hadCRUT4 (*green*), and the average of all three (*black*)

aerosol forcings resulting from anthropogenic emissions is highly uncertain (Forster et al. 2007). The uncertainty for the aerosol forcing is thus determined based on the uncertainty in the Intergovernmental Panel on Climate Change Fourth Assessment Report (IPCC AR4) for early 21st century aerosols. The direct aerosol forcing is sampled from a Gaussian distribution using a mean of $-0.5\ \mathrm{Wm}^{-2}$ and standard deviation of $0.2\ \mathrm{Wm}^{-2}$. A triangular distribution is used for the indirect aerosol forcing, due to the asymmetry in its uncertainty bounds, with a lower limit of $-1.8\ \mathrm{Wm}^{-2}$, an upper limit of $-0.3\ \mathrm{Wm}^{-2}$, and a mode of $-0.7\ \mathrm{Wm}^{-2}$. The forcings for the direct aerosol effect and indirect aerosol effect are sampled independently, as the present-day uncertainty in these quantities results more from the impact of these effects rather than the concentration of aerosols. For each sample, a scaling factor for aerosols is thus determined based on the ratio of this sampled early 21st century aerosol forcing to the aerosol forcing for the same time period in the GISS Model-E forcing data, which is then applied to aerosols throughout the record. The resulting net forcing change from 1955 to 2011 can be seen in Fig. 1b.

2.1.3 *Temperature data*

For surface temperatures, anomalies are taken as an average between three popular datasets: GISS land–ocean temperature index (Hansen et al. 2010), HadCRUT4 (Jones et al. 2012), and NCDC (Smith et al. 2008). Individual series and the combined average from 1955 to 2011 can be seen in Fig. 1c.

2.1.4 *Methodology*

From eq. 1, the calculation used here is:

$$\lambda_{50yr} = \frac{(F_{cur} - F_{hist}) - (N_{cur} - N_{hist})}{T_{cur} - T_{hist}} \tag{3}$$

where the subscript "cur" refers to the average for the quantity over one of the more recent periods, and "hist" refers to the 10-year average for that quantity over a specified historical period.

Both the "current" and historical period are varied when performing the estimate, which is important for a variety of reasons. First, there is a tradeoff between measurement uncertainty and internal variability, as an earlier historical period yields larger uncertainty in OHC estimates and forcing difference with the present, whereas a more recent historical period means that the differences with the present may be dominated more by internal variability and produce a value for λ that is not as relevant to longer timescales. Second, much of the historical period is dominated by volcanic eruptions that can produce spikes in the OHC data, yielding large sensitivities to the choice of start year (Fig. 2a). Third, natural variability may produce decades of anomalously low ocean heat uptake. Thus, by alternating both the start year for the historical period for each independent pentadal average, and the length of separation between the historical and current period to include every 5 year "climate-scale" (greater than 30 year) calculation, it is possible to get a more robust estimate for λ.

The estimated range for λ_{50yr} is obtained using Monte Carlo simulation, varying the start year for the current and historical period and determining N_{cur}, N_{hist}, F_{cur}, and F_{hist} based on the variable distributions described above.

Note that this approach differs from Gregory et al. (2002), who use an estimate for the historical net TOA imbalance over a period prior to the start of OHC observations—namely, they assume a near steady-state for the late nineteenth century and compare that to the heat flux from 1957 to 1994. As described in the above trade-off, such an approach consists of a longer timescale so as to ensure the calculated λ is less influenced by short-term variability, but it also requires modeling the heat flux in place of OHC observations in the late nineteenth century, and yields a larger uncertainty in the forcing difference between the two periods. Moreover, the approach here makes use of the latest OHC data up to 2012 and includes the 700–2,000 m layer.

2.2 Results

The resulting estimate for λ_{50yr} from the main analysis, including one standard deviation, is 2.05 ± 0.66 $Wm^{-2}K^{-1}$ (Fig. 2b). As can be seen in Fig. 2a, due to the asymmetric uncertainty surrounding anthropogenic aerosols (in particular, the indirect aerosol forcing), including this source of uncertainty generally decreases the estimate for the radiative restoration strength, thereby also increasing the diagnosed climate sensitivity. The lack of precision of ocean heat content estimates prior to the most recent decade also contributes greatly to the overall uncertainty using this method. With regards to the choice of dataset for upper ocean heat content, the Ishii and Kimoto (2009) set produces a similar estimate to the main analysis for λ_{50yr} of 1.96 $Wm^{-2}K^{-1}$, but using Domingues et al. (2008) results in a substantially lower estimate for λ_{50yr} of 1.45 $Wm^{-2}K^{-1}$, primarily because of the higher rate of upper ocean warming in that dataset for the most recent 15 years.

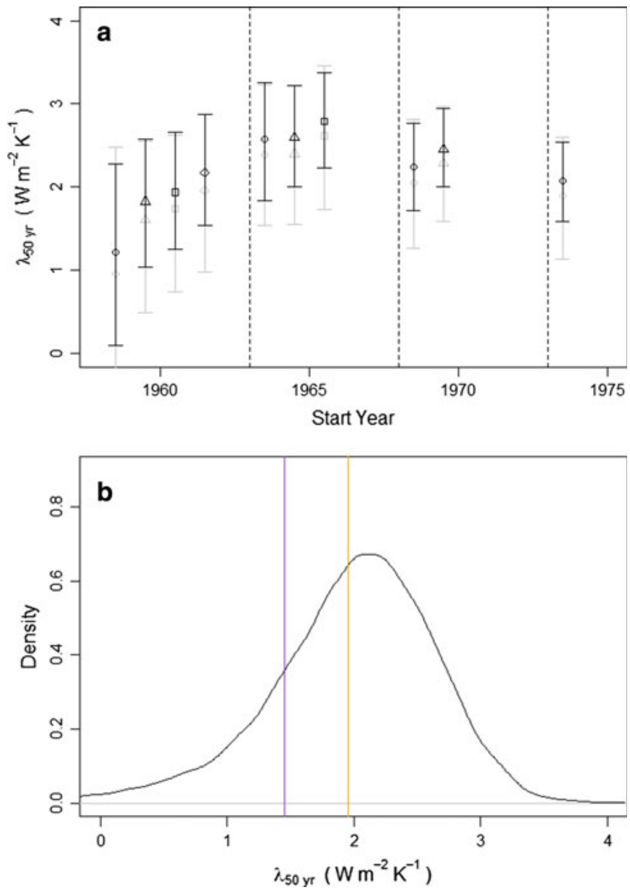

Fig. 2 **a** Median and 2.5–97.5 % confidence intervals for the radiative restoration strength (λ_{50yr}) for the main analysis according to the start year of the 10-year historical period used. Circles represent 30 years of separation between the historical and "current" period, triangles represent 35 years, squares represent 40 years, and the diamond represents 45 years. Median and confidence intervals in gray include uncertainty in the anthropogenic aerosol forcing, median and confidence intervals in black do not include it. **b** Probability distribution function for λ_{50yr}, using all start years and separation from (a) and all sources of uncertainty mentioned for the main analysis (*black*). Also included are the diagnosed likely values for λ_{50yr} when using Domingues et al. (*purple*) and Ishii and Kimoto (*orange*) for the UOHC dataset

3 Radiative response in CMIP3 models

3.1 Data and methods

An ensemble consisting of 32 model configurations and 76 members from the CMIP5 was used to study the relationship between λ_{50yr} and λ_{eff}, as well as to compare the radiative restoration strength over this period in the CMIP5 models to that obtained from the observations. These members were acquired from Climate Explorer (http://climexp.knmi.nl/; Van Oldenborgh et al. 2009) and additionally the variables used were drift-corrected using a Lowess smooth of the corresponding pre-industrial control experiments.

λ_{eff} has been calculated in the same manner as used by Soden and Held (2006). However, rather than using the A1B scenario that was available with the CMIP3 runs, the CMIP5 members used here come from the RCP 4.5 scenario (Taylor et al. 2012). Since this scenario is defined by a change in anthropogenic forcing of approximately 4.5 Wm^{-2} from the pre-industrial era by the year 2100, λ_{eff} is calculated according to Eq. 1 based on the difference between two 20-year averages of temperature and TOA radiation from years 1861–1880 and 2081–2100, along with the aforementioned change in forcing. There is some uncertainty in the 4.5 Wm^{-2} value due to the different radiative influence the various forcing agents may have in the different models examined. However, as the emissions of anthropogenic aerosols (black carbon, sulfate, etc.) largely decreases by the end of the 21st century in this scenario, the uncertainty in the net forcing when calculating λ_{eff} is far smaller than that of the present day net forcing.

λ_{50yr} has been estimated according to the same manner as in Sect. 2, except that the value for N is available from the AOGCM outputs without the measurement uncertainty present in the observations of ocean heat content. Similarly, λ_{50yr} is calculated by varying the start years and years of separation between the historical and "current" periods, then averaging the result for each member (Fig. 3). For F, the actual magnitude of the aerosol radiative forcing is not available for many of the CMIP models, so the same forcing history used in Sect. 2 is applied here. Since the underlying aerosol forcing that has actually been calculated for CMIP5 models can vary quite a bit (Shindell et al. 2012), using the same estimate for the aerosol forcing despite different underlying actual forcings for the models can highlight the impact this aerosol forcing can make on estimates of λ_{50yr}.

3.2 Results

The mean value for the ensemble is $\lambda_{50yr} = 1.16$ $Wm^{-2}K^{-1}$, with a standard deviation of 0.52 $Wm^{-2}K^{-1}$. The mean value of λ_{50yr} if each model configuration is weighted equally (rather than weighting each run equally) is 1.18 $Wm^{-2}K^{-1}$. Of the 76 members used, 16 members (8 model configurations) result in a calculated λ_{50yr} that is within one standard deviation of the best estimate from the main analysis observations. Only 3 members produce a value for λ_{50yr} that is higher than the best estimate value from observations, with the remainder falling below. The two models with the highest value for λ_{50yr} are INM-CM4 and MRI-CGCM3, which, as expected, are among the least sensitive models from the CMIP5 ensemble, with diagnosed ECS of 2.1 and 2.6 K respectively [Andrews et al. 2012]. The other run that shows a higher λ_{50yr} than the best estimate from observations comes from CSIRO-Mk-3-6-0, which has a larger sensitivity (4.1 K), although this particular model shows the largest range of variability in λ_{50yr} across runs and also includes 9 more runs that fall below this estimate, including four that fall below the lower bound from observations. Moreover, CSIRO-Mk-3-6-0 includes a larger influence from anthropogenic aerosols than most of the other CMIP5 models for which this information is available (Shindell et al. 2012), thereby making the diagnosed sensitivity appear lower when the larger efficacy of these aerosol forcings is not taken into account. 12 of the models examined include multiple runs. As mentioned previously, CSIRO-Mk-3-6-0 shows the largest variation in λ_{50yr} across runs ($\sigma = 0.39$ $Wm^{-2}K^{-1}$), while CanESM2 shows the least ($\sigma = 0.04$ $Wm^{-2}K^{-1}$).

Figure 4 shows the relationship between the mean 30–50 year radiative restoration strength (λ_{50yr}) and the effective restoration strength (λ_{eff}) in the 32 models used. The result (r = 0.50) indicates that there is a strong relationship between the radiative restoration strength of the last half-century and the longer-term effective sensitivity. This relationship may be somewhat surprising, given that the exact model forcings are not used when determining λ_{50yr}, and shows that there is information to be gleaned from the change in heat flux imbalance and surface temperatures even if the exact forcings are unknown. However, the average model effective restoration strength (λ_{eff}) is 1.44 $Wm^{-2}K^{-1}$, substantially larger than the average model value for λ_{50yr} of 1.18 $Wm^{-2}K^{-1}$. This method of determining effective sensitivity from the transient state of the RCP 4.5 scenario seems to yield a larger value for (λ_{eff}) than when determining this climate feedback parameter (α) using a similar method with the abrupt 4xCO_2 scenario (Andrews et al. 2012). In fact, the average model value for λ_{50yr} of 1.18 $Wm^{-2}K^{-1}$ seems to match the model average for α of 1.08 $Wm^{-2}K^{-1}$ obtained from Andrews et al. (2012) better than λ_{eff} here, although different sets of models were examined and this result may be mere coincidence.

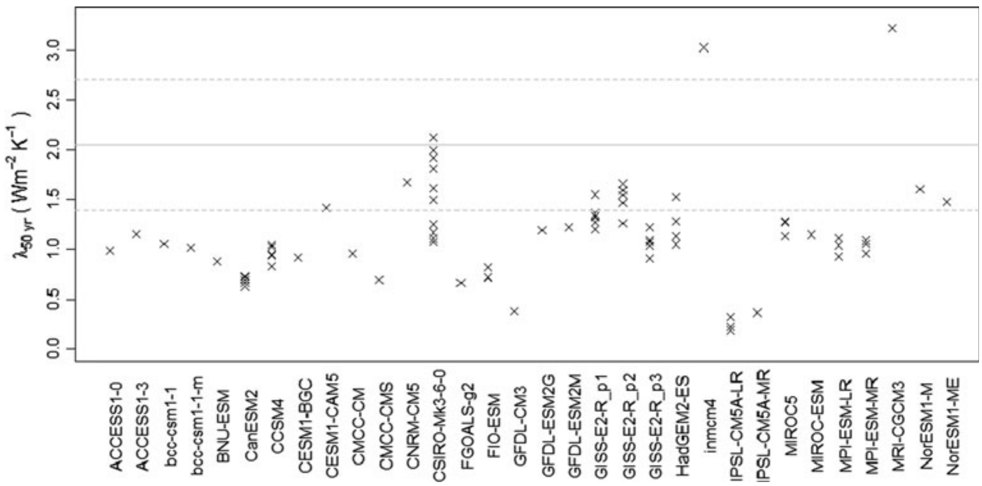

Fig. 3 Resulting estimates for λ_{50yr} from the CMIP5 models. The median value of λ_{50yr} from observations is included (*solid gray*) along with ±1 standard deviation (*dashed gray*)

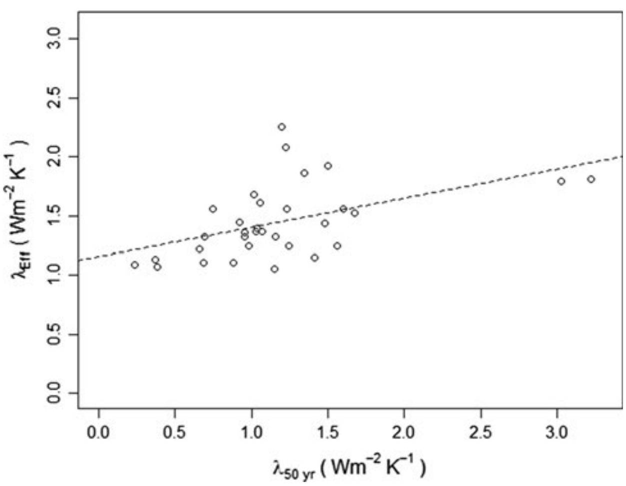

Fig. 4 Plot of the mean λ_{50yr} against the mean λ_{eff} for the CMIP5 models used (r = 0.50)

4 Estimating equilibrium climate sensitivity

4.1 Data and methods

The resulting pdf of λ_{50yr} from Sect. 2 (Fig. 2b) is used as the starting point for λ in Eq. 1 to produce resulting estimates of equilibrium climate sensitivity. However, although using λ_{50yr} clearly appears to be at least somewhat indicative of longer-term sensitivity, there is also evidence to suggest some uncertainty in the relationship between these multi-decade to century scale radiative restoration strengths and the strength of the radiative restoration calculated after equilibrium is reached (λ_{eq}) (Winton et al. 2010). Since the latter state can take several hundred to thousands of years to reach, this value is not available for many models in the CMIP5 archive. However, Table 1 highlights the relationship between λ_{eq} and λ_{eff} in several of the CMIP3 models, for which λ_{eq} has already been calculated. Obviously, the λ_{50yr} calculated here is not completely analogous to the λ_{eff} determined for those CMIP3 models, given the larger forcing change and timescale of the latter. It is also debatable whether the relationship between λ_{eq} and λ_{eff} in those models should serve to indicate the probability distribution of $\lambda_{eq}/\lambda_{50yr}$ given the apparent bias in AOGCMs shown above. For this reason, Fig. 5 also includes a pdf for ECS when λ is assumed to be constant after approximately 30 years ($\lambda_{eq} = \lambda_{50yr}$). Nevertheless, for the main analysis, it is believed that at least some variation in the relationship between the radiative restoration strength on these longer timescales exists and should be reflected in the estimate. The value of $\lambda_{eq}/\lambda_{50yr}$ is thus sampled from a Gaussian distribution, with a mean of 1.09 and standard deviation of 0.20 based on the relationship in Table 1, when performing the Monte Carlo simulations to produce the resulting pdf for ECS, and the value of 3.7 Wm^{-2} is used for ΔF_{2xCO2}.

Table 1 Relationship between λ_{eff} and λ_{eq} in CMIP3 models

AOGCM	λ_{eff} ($Wm^{-2}K^{-1}$)	λ_{eq} ($Wm^{-2}K^{-1}$)	$\lambda_{eff}/\lambda_{eq}$
GFDL CM2.0	1.18	1.21	0.98
GFDL CM2.1	1.37	1.03	1.33
GISS ER	1.64	1.50	1.09
IPSL	0.98	0.79	1.24
MIROC MEDRES	0.91	0.77	1.18
MRI	1.5	1.08	1.38
MPI ECHAM5	0.88	1.18	0.75
NCAR CCSM3	1.62	1.46	1.11
NCAR PCM1	1.53	1.71	0.89
UKMO HADCM3	0.97	1.00	0.97
Mean			1.09
Std Dev			0.20

λ_{eff} is from Table 1 of Soden and Held (2006), while λ_{eq} is calculated from R and T_{eq} in Table 2 of Winton et al. (2010)

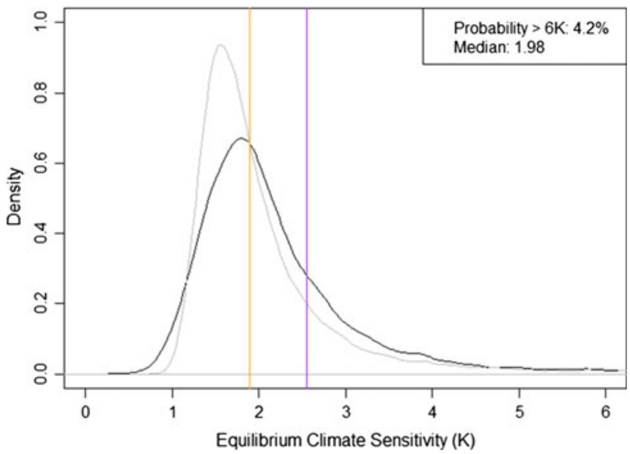

Fig. 5 The resulting probability distribution for the equilibrium climate sensitivity as diagnosed from the main analysis observations (*black*), as well as the pdf for the main analysis if λ_{50yr} is assumed to be equal to λ_{eq} (*gray*). Point estimates for the most likely value when using Domingues UOHC (*purple*) and Ishii and Kimoto *UOHC* (*orange*) are also shown

4.2 Results

This method yields a median estimate for ECS of 1.98 K, with a likely (67 %) range of 1.47–2.95 K and a 90 % confidence interval of 1.19–5.15 K. Including all sources of uncertainty mentioned—anthropogenic aerosol estimates, OHC measurements, ocean heat uptake percent, and potential non-linearity of sensitivity in the temperature domain ($\lambda_{eq} \neq \lambda_{eff}$)—yields a potential of ECS exceeding 6 K of about 4.2 %, although such a possibility in this analysis primarily results from one 1960,1990 current/historical start year pairing, as the combined ocean heat content data uncertainty in that pairing yields extremely large bounds for λ_{50yr}.

As can be seen in Fig. 5, including the distribution for the $\lambda_{eq}/\lambda_{50yr}$ slightly increases the median ECS from 1.79 to 1.98 K, but otherwise serves more to widen the potential range of ECS, as the unmodified pdf corresponds to a 90 % confidence interval of 1.24–4.29 K. As expected, using Ishii and Kimoto (2009) UOHC yields a most likely ECS close to the median in the main analysis, while using Domingues et al. (2008) UOHC yields a most likely ECS of 2.55 K that is slightly higher, but still falls within the likely range of the main analysis.

5 Summary and discussion

From the 32-model CMIP5 ensemble examined, it is clear that the method of using the most recent $\sim$50 years of heat flux and temperature data, along with estimates for the radiative forcing, indicates a good correlation between the radiative restoration strength (λ_{50yr}) diagnosed over the transient period and the value calculated over multiple-centuries (λ_{eff}). Furthermore, as expected, the models that produce the largest values of λ_{50yr} exhibit the least temperature sensitivity to a doubling of CO_2.

The observational estimate for climate sensitivity of 1.98 K [1.19–5.15 K] produced by this method is slightly lower than that of the IPCC AR4 (3 K [2–4.5 K]) (Hegerl et al. 2007), as well as the range of CMIP5 models (Andrew et al. 2012). The latter is not surprising given that only three of the CMIP5 members examined matched or exceeded the median strength of radiative restoration (λ_{50yr}) as diagnosed from observations, and they generally produce a value for λ_{50yr} that appears to be biased low. This would seem to suggest that most of the CMIP5 AOGCMs examined here generally show too much temperature sensitivity, although there are several other potential factors that may be involved: first, if the magnitude of the negative aerosol forcing at present day is towards the upper extreme of the IPCC AR4 estimate, this would have masked even more of the GHG forcing and a revised estimate would include higher sensitivities (similarly, an aerosol forcing with a magnitude toward the lower range would suggest a lower sensitivity). Schwartz (2012) notes a similar dependence on the underlying aerosol forcing. Second, it may be that most AOGCMs do not properly represent the non-linearity of the temperature response in the transient climate states. For instance, if $\lambda_{50yr}/\lambda_{eq} \gg 1$ due to an increase in the strength of certain positive feedbacks with temperature, diagnosing ECS in this manner would produce a significant underestimate. Armour et al. (2012) suggests that the actuation of different strength regional feedbacks by the evolution of surface warming patterns over time may be responsible for such a relationship. Third, it is possible that unforced natural variation (perhaps in the horizontal warming pattern) has contributed to an anomalously low radiation imbalance in recent decades. Finally, the Domingues et al. (2008) upper ocean heat content dataset produces a substantially lower λ_{50yr} than the other two datasets, which would remove some of the discrepancy between the AOGCMs and observations, although the best estimate of 1.45 $Wm^{-2}K^{-1}$ using that dataset is still above the ensemble mean of 1.16 $Wm^{-2}K^{-1}$.

Several other recent estimates of ECS have also been based on simple conceptual models and climate state observations. Aldrin et al. (2012) use hemispheric temperatures, 0–700 m OHC data, and a simple energy-balance climate/upwelling diffusion ocean model to produce an estimate of 1.98 K [1.07–4.28 K] for ECS, a result similar to that of this paper. Lin et al. (2010) use a conceptual model that includes climate system memory and deep ocean heat transport when estimating ECS from the current TOA imbalance and the temperature evolution of the 20th century, finding a best match for ECS of 3.1 K. However, they note that this is contingent upon the assumed TOA imbalance of 0.85 Wm^{-2}; using a more recent estimate of 0.5 Wm^{-2} (Loeb et al. 2012) results in the Lin et al. (2010) method producing an estimate more in-line with this paper and Aldrin et al. (2012). Schwartz (2012) produces a likely range for ECS of 1.16–4.9 K that is similar to the range found here, using a two-compartment energy balance model and similar observations over the 20th century.

The method used in this paper differs from these others in that it does not require fitting additional parameters, such as the mixed layer heat capacity or ocean diffusion rate, and explicitly includes uncertainty for the relationship between λ_{eff} and λ_{eq} as derived from CMIP3 models. While this estimate cannot be considered as independent from these others due to the overlap in datasets used (ocean heat content and surface temperature during the 20th and 21st century), the focus on the *change* in the ocean heat uptake rate over the course of OHC observations provides an additional approach.

Acknowledgments I would like to thank Geert Jan van Oldenborgh at KNMI for creating and maintaining the Climate Explorer website from which the CMIP5 members were retrieved (http://climexp.knmi.nl/) and aiding in the acquisition of this data. I also want to acknowledge Gavin Schmidt for comments on model drift, Urs Beyerle for help accessing the ETHZ CMIP5 sub-archive, Jonathan Gregory for information on CMIP5 run ancestry, and Catia Domingues for updates and comments on their latest UOHC data. Finally, I thank the two anonymous reviewers for helpful comments on this manuscript.

References

Aldrin M, Holden M, Guttorp P, Skeie RB, Myhre G, Berntsen TK (2012) Bayesian estimation of climate sensitivity based on a simple climate model fitted to observations of hemispheric temperatures and global ocean heat content. Environmetrics 23(3):253–271. doi:10.1002/env.2140

Andrews T, Gregory JM, Webb MJ, Taylor KE (2012) Forcing, feedbacks and climate sensitivity in CMIP5 coupled atmosphere-ocean climate models. Geophys Res Lett 39(9):L09712

Annan JD, Hargreaves JC (2006) Using multiple observationally-based constraints to estimate climate sensitivity. Geophys Res Lett 33(6):L06704

Armour KC, Bitz CM, Roe GH (2012) Time-varying climate sensitivity from regional feedbacks. J Clim. doi:10.1175/JCLI-D-12-00544.1

Church JA, White NJ, Konikow LF, Domingues CM, Cogley JG, Rignot E, Gregory JM, van den Broeke MR, Monaghan AJ, Velicogna I (2011) Revisiting the Earth's sea-level and energy budgets from 1961 to 2008. Geophys Res Lett 38:L18601. doi:10.1029/2011GL048794

Colman RA, Hanson LI (2012) On atmospheric radiative feedbacks associated with climate variability and change. Clim Dyn 40(1):475–492

Domingues CM, Church JA, White NJ, Gleckler PJ, Wijffels SE, Barker PM, Dunn JR (2008) Improved estimates of upper-ocean warming and multi-decadal sea-level rise. Nature 453(7198): 1090–1093

Edwards TL, Crucifix M, Harrison SP (2007) Using the past to constrain the future: how the palaeorecord can improve estimates of global warming. Prog Phys Geogr 31(5):481–500

Forster P, Ramaswamy V, Artaxo P, Berntsen T, Betts R, Fahey DW, Haywood J, Lean J, Lowe DC, Myhre G, Nganga J, Prinn R, Raga G, Schulz M, Van Dorland R (2007) Changes in Atmospheric Constituents and in Radiative Forcing. In: Solomon S, Qin D, Manning M, Chen Z, Marquis M, Averyt KB, Tignor M, Miller HL (eds) Climate Change 2007: The Physical Science Basis Contribution of Working Group I to the Fourth Assessment Report of the Intergovernmental Panel on Climate Change. Cambridge University Press, Cambridge

Forster PMF, Gregory JM (2006) The climate sensitivity and its components diagnosed from Earth radiation budget data. J Clim 19(1):39–52

Gregory JM, Stouffer RJ, Raper SCB, Stott PA, Rayner NA (2002) An observationally based estimate of the climate sensitivity. J Clim 15(22):3117–3121

Hansen J, Sato M, Ruedy R, Kharecha P, Lacis A, Miller et al (2007) Climate simulations for 1880–2003 with GISS modelE. Clim Dyn 29(7):661–696

Hansen J, Ruedy R, Sato M, Lo K (2010) Global surface temperature change. Rev Geophys 48:RG4004. doi:10.1029/2010RG000345

Hegerl GC, Zwiers FW, Braconnot P, Gillett NP, Luo Y, Marengo Orsini JA, Nicholls N, Penner JE, Stott PA (2007) Understanding and attributing climate change. In: Solomon S, Qin D, Manning M, Chen Z, Marquis M, Averyt KB, Tignor M, Miller HL (eds) Climate change 2007: the physical science basis contribution of working group I to the fourth assessment report of the intergovernmental panel on climate change. Cambridge University Press, Cambridge

Held IM, Winton M, Takahashi K, Delworth T, Zeng F, Vallis GK (2010) Probing the fast and slow components of global warming by returning abruptly to preindustrial forcing. J Clim 23(9):2418–2427

Ishii M, Kimoto M (2009) Reevaluation of historical ocean heat content variations with time-varying XBT and MBT depth bias corrections. J Oceanogr 65(3):287–299

Jones PD, Lister DH, Osborn TJ, Harpham C, Salmon M, Morice CP (2012) Hemispheric and large-scale land-surface air temperature variations: an extensive revision and an update to 2010. J Geophys Res 117:D05127. doi:10.1029/2011JD017139

Knutti R, Hegerl GC (2008) The equilibrium sensitivity of the Earth's temperature to radiation changes. Nat Geosci 1(11):735–743

Levitus S et al (2012) World ocean heat content and thermosteric sea level change (0–2,000 m), 1955–2010. Geophys Res Lett 39:L10603. doi:10.1029/2012GL051106

Lin B, Chambers L, Stackhouse P Jr, Wielicki B, Hu Y, Minnis P et al (2010) Estimations of climate sensitivity based on top-of-atmosphere radiation imbalance. Atmos Chem Phys 10: 1923–1930

Lin B, Min Q, Sun W, Hu Y, Fan TF (2011) Can climate sensitivity be estimated from short-term relationships of top-of-atmosphere net radiation and surface temperature? J Quant Spectrosc Radiat Transfer 112(2):177–181

Lindzen RS, Choi YS (2011) On the observational determination of climate sensitivity and its implications. Asia-Pacific J Atmos Sci 47(4):377–390

Loeb NG, Lyman JM, Johnson GC, Allan RP, Doelling DR, Wong T et al (2012) Observed changes in top-of-the-atmosphere radiation and upper-ocean heating consistent within uncertainty. Nat Geosci 5(2):110–113

Mascioli NR, Canty T, Salawitch RJ (2012) An empirical model of global climate-part 2: implications for future temperature. Atmos Chem Phys Discuss 12:23913–23974. doi:10.5194/acpd-12-23913-2012

Murphy JM, Sexton DM, Barnett DN, Jones GS, Webb MJ, Collins M, Stainforth DA (2004) Quantification of modelling uncertainties in a large ensemble of climate change simulations. Nature 430(7001):768–772

Murphy DM, Solomon S, Portmann RW, Rosenlof KH, Forster PM, Wong T (2009) An observationally based energy balance for the Earth since 1950. J Geophys Res 114(D17):D17107

Schwartz SE (2012) Determination of Earth's transient and equilibrium climate sensitivities from observations over the twentieth century: strong dependence on assumed forcing. Surveys Geophys 33:745–777. doi:10.1007/s10712-012-9180-4

Shindell DT, Lamarque JF, Schulz M, Flanner M, Jiao C, Chin M, Yoon JH (2012) Radiative forcing in the ACCMIP historical and future climate simulations. Atmos Chem and Phys Discuss 12:21105–21210

Smith TM, Reynolds RW, Peterson TC, Lawrimore J (2008) Improvements to NOAA's historical merged land-ocean surface temperature analysis (1880–2006). J Clim 21:2283–2293. doi:10.1175/2007JCLI2100.1

Soden BJ, Held IM (2006) An assessment of climate feedbacks in coupled ocean-atmosphere models. J Clim 19(14):3354–3360

Taylor KE, Stouffer RJ, Meehl GA (2012) An overview of CMIP5 and the experiment design. Bull Am Meteorol Soc 90:485–498. doi:10.1175/BAMS-D-11-00094.1

Van Oldenborgh GJ, Drijfhout S, Van Ulden A, Haarsma RJ, Sterl A, Severijns C, Dijkstra HA (2009) Western Europe is warming much faster than expected. Climate of the Past 5(1):1–12

Winton M, Takahashi K, Held IM (2010) Importance of ocean heat uptake efficacy to transient climate change. J Clim 23(9):2333–2344